Available online at www.sciencedirect.com
SCIENCE DIRECT
Journal of the European Ceramic Society 26 (2006) 117–123
www.elsevier.com/locate/jeurceramsoc

Preparation of sub-micron PZT particles with the sol–gel technique

S. Linardos*, Q. Zhang, J.R. Alcock

Advanced Materials Department, School of Industrial and Manufacturing Science, Cranfield University, Bedfordshire MK430AL, UK

Received 18 May 2004; received in revised form 23 September 2004; accepted 1 October 2004
Available online 13 December 2004

Abstract

This paper describes the production of $Pb_{1.0}Zr_{0.9}Ti_{0.1}$ ceramic powder, by using metal organic precursors as starting materials. In this study polyvinylpyrrolidone, PVP, was used to create a PZT–PVP sol and then also added as a secondary stage to control the particle size of the powder.

Two different sol–gel routes were used to create PZT powder. Both routes gave similar primary particle sizes in the range, 30–70 nm, but different agglomerate formations. Perovskite PZT powder was created with both routes.

Keywords: Powders-chemical preparation; Sol–gel processes; PZT

1. Introduction

In advanced ceramics the size, size distribution, shape and state of agglomeration of the starting powder strongly affect the microstructure of the sintering body, and the temperature at which it densifies.[1]

Lead zirconate titanate (PZT) is an important ferroelectric material, widely used for its piezoelectric and pyroelectric properties. There are a variety of methods for the preparation of PZT powder. Mechanochemical synthesis[2–5], chemical synthesis[6–10] or hydrothermal synthesis[11–14] has each been successfully used.

Processing routes for the production of monodispersed fine powders are becoming increasingly common. TiO_2, ZrO_2 and SiO_2 were some of the first powders to have been successfully created[15–19] with the sol–gel technique. The synthetic methods used to prepare these materials involve fairly simple solution chemistry, however, they give a high degree of control and reproducibility.

However, it is more difficult to create monodispersed particles with two or more metallic elements because of the tendency of one of the metal alkoxides to precipitate out of the solution more quickly than the other. This is owing to differences in hydrolysis rates of the alkoxides.

A sol–gel technique has previously been used by several authors[20–26] to create a PZT powder.

In this paper a new sol–gel route for PZT, incorporating polyvinylpyrrolidone, PVP, is presented. PVP has previously been used with success for the creation of crack free thick, and thin films[27,28] and in some cases to improve the properties of the final powders.[29,30] In this study PVP, was used both to create a PZT–PVP sol and also as a secondary stage to control the particle size of the powder produced.

The advantage of this new sol–gel route is the capability of producing controlled nano-scale ceramic powder with specific crystalline phase.

2. Experimental

The preparation route of the $Pb_{1.0}Zr_{0.9}Ti_{0.1}$–PVP gel (i) is shown in Fig. 1.

To produce 160 ml of sol, the following route was used. 12.14 g of lead(II) acetate trihydrate was left under vacuum at 100 °C for 24 h to remove the water. 12.21 g of zirconium(IV) propoxide, 76.33% by weight in *n*-propanol, and

* Corresponding author. Fax: +44 1234 752473.
E-mail addresses: s.linardos.2001@cranfield.ac.uk (S. Linardos), j.r.alcock@cranfield.ac.uk (J.R. Alcock).

0955-2219/$ – see front matter © 2004 Elsevier Ltd. All rights reserved.
doi:10.1016/j.jeurceramsoc.2004.10.007

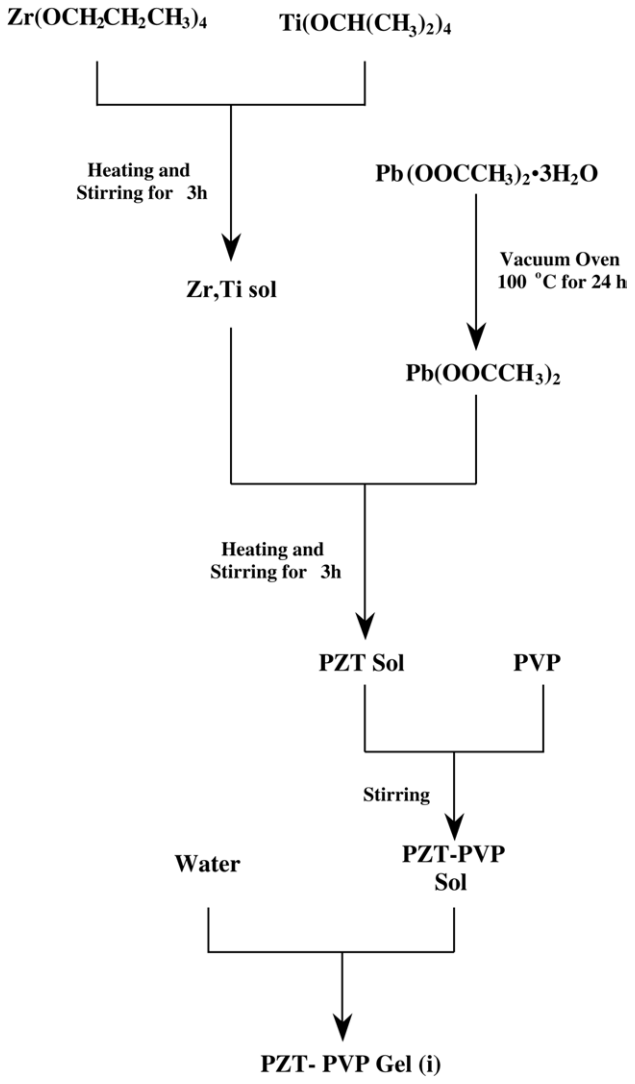

Fig. 1. Preparation route of PZT–PVP gel.

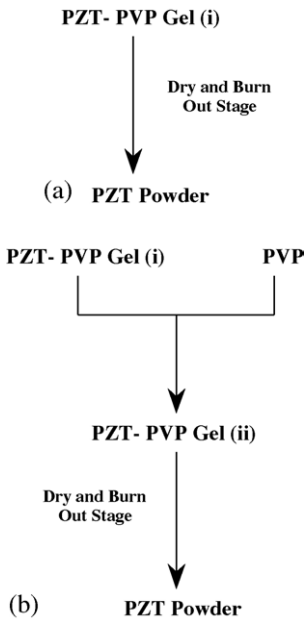

Fig. 2. (a) Preparation route A for PZT powder. No PVP was added as a secondary stage. (b) Preparation route B for PZT powder. PVP was added as a secondary stage.

0.9 g of titanium(IV) isopropoxide were dissolved in 120 ml isopropanol. This mixture was heated to 80 °C under stirring. After three hours the lead(II) acetate was added. The mixture was stirred for another three hours under the same conditions. Extra isopropanol was added until the final volume of the solution reached the 160 ml. A light-transparent PZT sol was obtained. To transform this into a PZT–PVP sol, 5.5 g of PVP with average molecular weight of 1,300,000 were added and the stirring was continued until it became clear yellow in colour.

The resulting PZT–PVP sol had a concentration of 0.2 M of lead. The $Pb(OAc)_2$: PVP weight ratio of the sol was 1:0.5. In order to hydrolyse this to produce a gel, water was slowly added up to the maximum of $[H_2O]/[Pb] = 0.66$. A PZT–PVP gel, gel (i), was obtained.

Subsequent to these common processing steps, two processing routes, here called A and B were followed.

Powder preparation route A is shown in Fig. 2a. The PZT–PVP gel (i) was left to dry at 60 °C for 144 h and then burnt out at 500 °C for 1 h. An orange coloured powder was created.

Powder preparation route B is shown in Fig. 2b. The PZT–PVP gel (i) was stirred for 10 min at 1200 rpm, and then 0.2 g of PVP with average molecular weight 55,000 was added per millilitre of sol. The new PZT–PVP gel, gel (ii), was dried at 60 °C for 144 h and then heat treated at two different profiles, one at 500 °C for 1 h and the second at 550 °C for 24 h.

A Philips XL series scanning electron microscope and a Siemens D5005 X-ray diffractometer were used for sample analysis.

Size measurements of the powder were performed using a Zeta-Sizer 3000 (Malvern Instruments). Each powder before the measurements was diluted in water and left in an ultrasound bath for 40 min.

Differential scanning calorimetry of the gels was performed using a modulated DSC (TA Instruments) model 2920. A constant heating rate of 10 °C min^{-1} from 20 to 450 °C was used, with an isothermal dwell at 450 °C for 60 min. All the measurements took place under a constant nitrogen flow. Hermetic aluminium pans were used to encapsulate the samples.

3. Results

Fig. 3a and b are SEM micrographs of typical PZT powder that was produced using route A. In Fig. 3a non-spherical particulates of the order of 10 μm in size can be observed. Fig. 3b shows a higher magnification micrograph of the surface of a particulate. It indicates that the 10 μm sized ag-

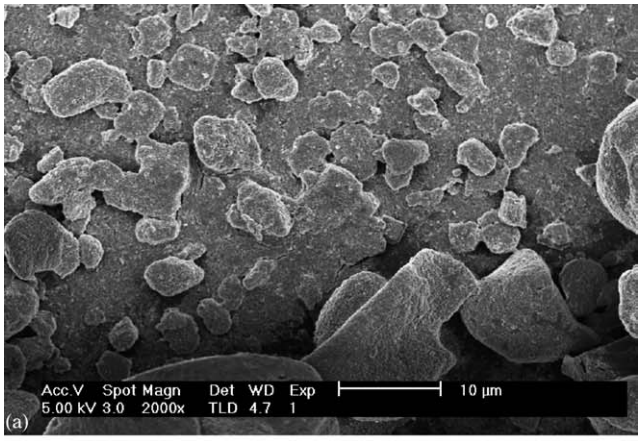

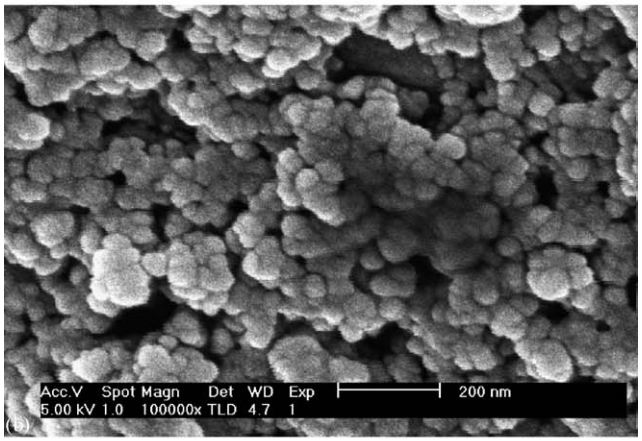

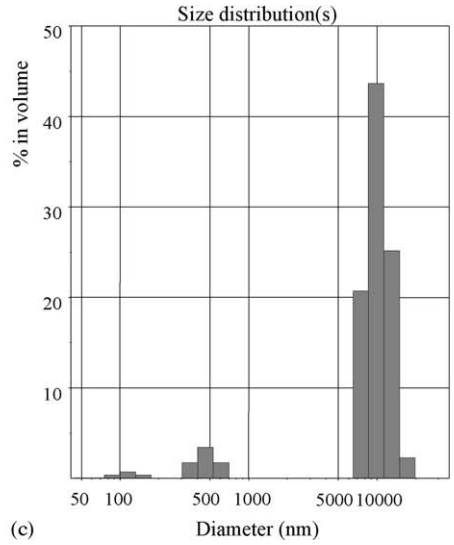

Fig. 3. (a) SEM micrograph of PZT powder. No PVP was added as secondary stage. Burn out at 500 °C for 1 h. (b) SEM micrograph of PZT powder. No PVP was added as secondary stage. Burn out at 500 °C for 1 h. (c) Size distribution in volume of PZT powder. No PVP was added as secondary stage. Burn out at 500 °C for 1 h.

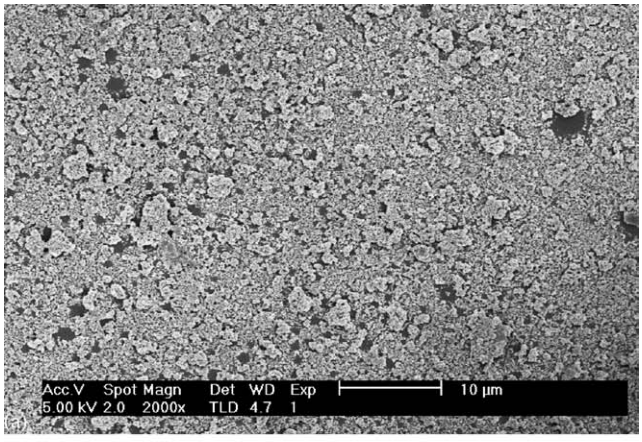

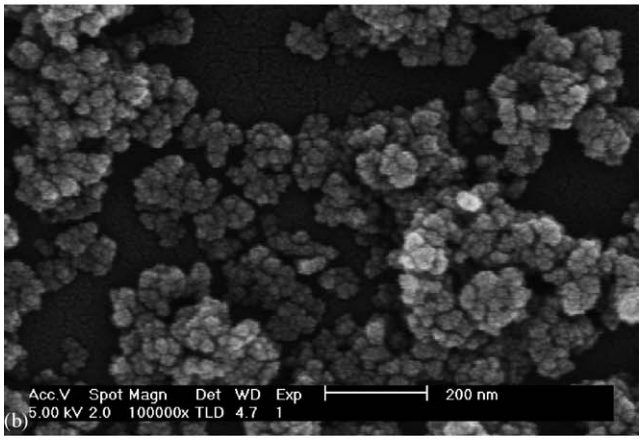

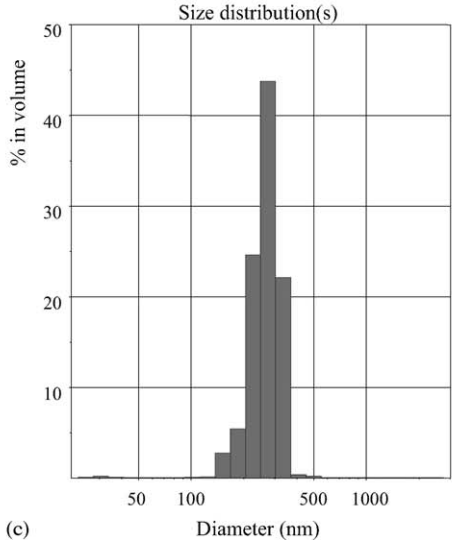

Fig. 4. (a) SEM micrograph of PZT powder. PVP added as secondary stage. Burn out at 500 °C for 1 h. (b) SEM micrograph of PZT powder. PVP added as secondary stage. Burn out at 500 °C for 1 h. (c) Size distribution in volume of PZT powder. PVP added as secondary stage. Burn out at 500 °C for 1 h.

glomerates are composed of primary particles of particle size 30–70 nm.

Fig. 3c is a volume percent against particle diameter histogram of PZT powder that was produced with route A. The diagram show that almost 90% in volume of the powder consisted of particles with diameter above 5 μm and only 10% in volume of the powder consists from sub-micron particles.

Fig. 4a and b are SEM micrographs of examples of PZT powder that was produced using route B and subse-

quently heat treated at 500 °C for 1 h. In Fig. 4a, particle agglomerates of up to 3 μm in size with an approximately equiaxed shape can be observed. Fig. 4b shows a higher magnification micrograph of free standing agglomerates with diameter 50–200 nm and primary particle size 30–50 nm.

Fig. 4c is a particle diameter histogram of PZT powder that was produced using route B and subsequently heat treated at 500 °C for 1 h. The diagram shows that only sub-micron particle formations were detectable in the suspension. The average diameter of particles formations in water is around 250 nm.

Fig. 5a and b are SEM micrographs of examples of PZT powder that was produced using route B and heat treated at 550 °C for 24 h. Fig. 5a shows agglomerates up to 2 μm in diameter with approximately equiaxed shape. The higher magnification micrograph, Fig. 5b, shows agglomerated primary particles with a primary particle size similar to the 500 °C heat treated powder.

Fig. 5c is a particle diameter histogram of PZT powder that was produced using route B and heat treated at 550 °C for 24 h. The diagram shows that around 95% of the total volume of the powder consist from sub-micron formations with mean diameter around 350 nm. About 5% of the powder volume consists from particles with size 2–3 μm.

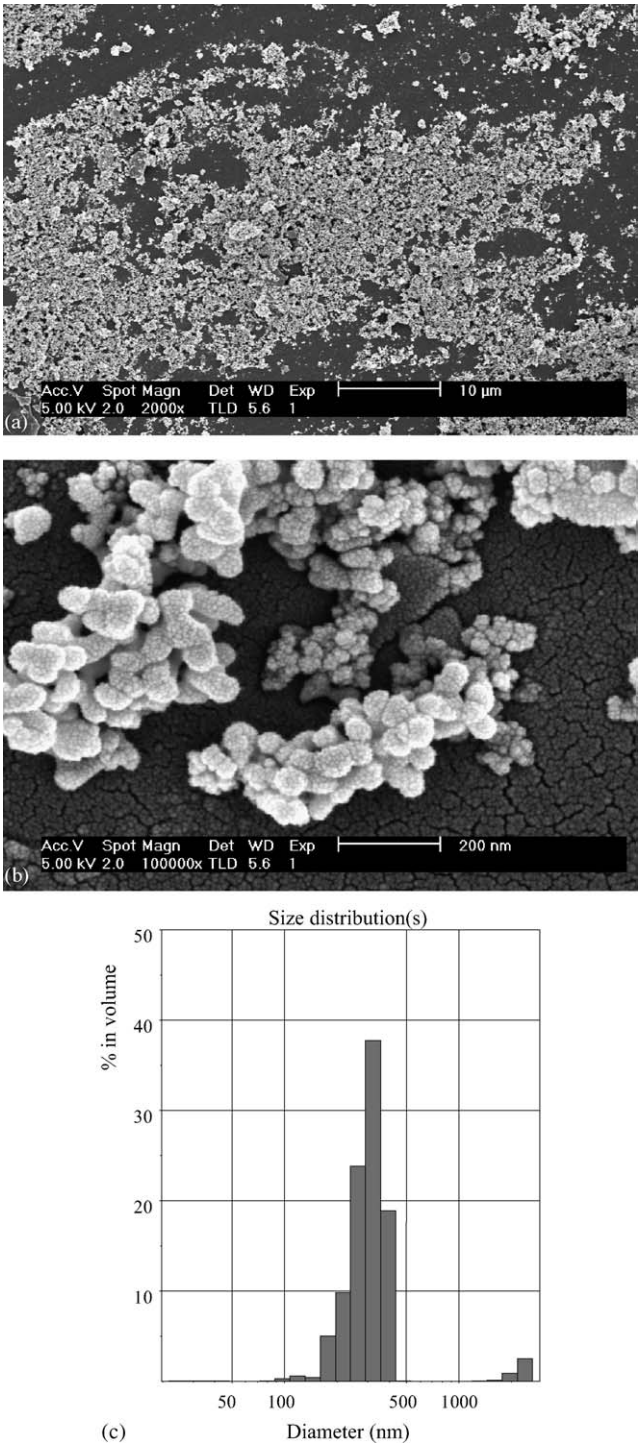

Fig. 5. (a) SEM micrograph of PZT powder. PVP added as secondary stage. Burn out at 550 °C for 24 h. (b) SEM micrograph of PZT powder. PVP added as secondary stage. Burn out at 550 °C for 24 h. (c) Size distribution in volume of PZT powder. PVP added as secondary stage. Burn out at 550 °C for 24 h.

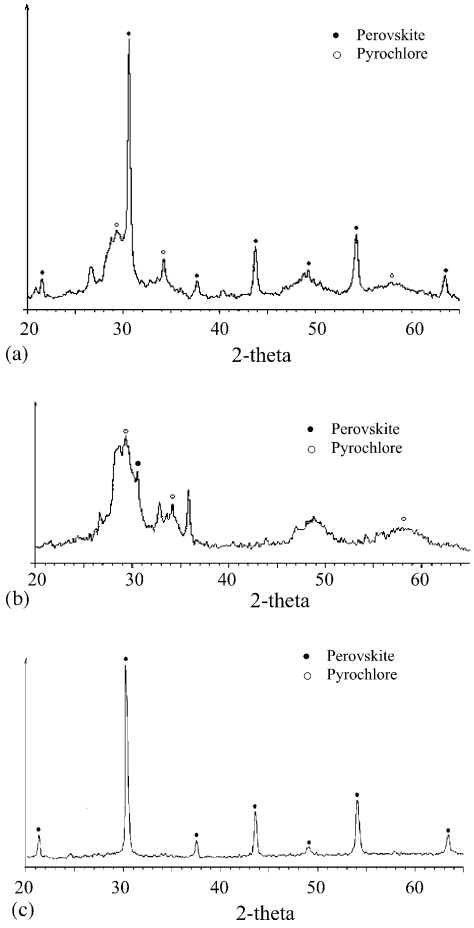

Fig. 6. (a) XRD diagram of PZT powder. No PVP was added as secondary stage. Burn out at 500 °C for 1 h. (b) XRD diagram of PZT powder. PVP added as secondary stage. Burn out at 500 °C for 1 h. (c) XRD diagram of PZT powder. PVP added as secondary stage. Burn out at 550 °C for 24 h.

Fig. 6a–c are XRD diagrams of PZT powders that were produced with routes A and B. In Fig. 6a, an XRD diagram of PZT powder produced with route A and heat treated at 500 °C for 1 h is presented. Comparison with the peaks for pyrochlore and perovskite shows that this route powder is a mixture of pyrochlore and perovskite phases. Fig. 6b is a XRD diagram of PZT powder produced with route B and heat treated at 500 °C for 1 h. This is mainly pyrochlore with very little perovskite phase present. In Fig. 6c, an XRD diagram of PZT powder produced with route B and heat treated at 550 °C for 24 h is presented. The XRD peaks show that this heat treatment gave a powder with perovskite phase only.

Fig. 7a shows heat flow against time curves for the PZT sol and the 1,300,000 MW PVP, respectively. The PZT-sol exhibits a shallow endothermic peak between 50–140 °C followed by two broad exothermic peaks, one at 310–350 °C and the second at 420–450 °C. The 1,300,000 MW PVP, exhibits two endothermic peaks one at 50–100 °C and the second at 420–440 °C. Fig. 7b shows heat flow diagrams for gel (i) and gel (ii). Gel (i) exhibits two exothermic peaks one at 320–370 °C and the second at 410–450 °C. Gel (ii) also exhibits two endothermic peaks, one at 40–150 °C, and the second at 410–450 °C, as well as two exothermic peaks, the first at 320–370 °C and the second at 420–450 °C.

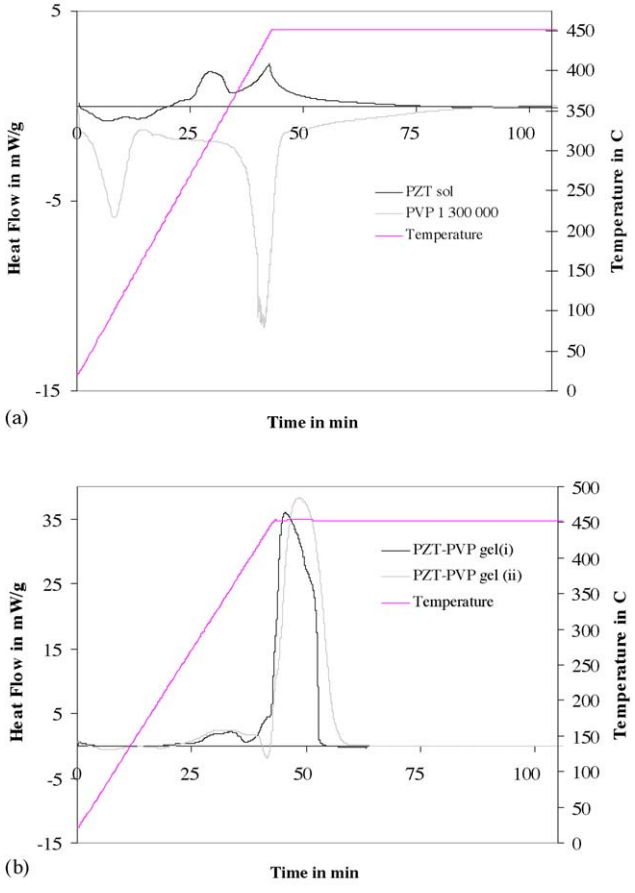

Fig. 7. (a) DSC diagrams of PZT sol and PVP polymer with average molecular weight 1,300,000. (b) DSC diagrams of PZT–PVP gel (i) and PZT–PVP gel (ii).

4. Discussion

From the SEM micrographs it can be observed that all three powders have the same size range of primary particles diameter 30–50 nm. It can be concluded that the extra polymer that was added in the secondary process stage did not significantly affect the size of the primary particles. However, a comparison of Figs. 3a and c and 4a and c indicates that the second addition of polymer significantly reduces the agglomerate size.

Comparing the results, it can be hypothesised that by adding extra polymer, as a secondary stage, the PZT particles in the gel were immobilized. As a consequence of this immobilization, the particles were hindered from reacting and creating agglomerated formations of larger particles during the drying and burn out steps. C=O groups of PVP are known to be strongly bonded with OH groups of the metalloxane polymers via hydrogen bonding.[31,32] Such C=O groups can be regarded as the "capping agent" for the OH groups of the metalloxane polymers, obstructing the condensation reaction.

A comparison between XRD Fig. 6a and b shows that similar conditions in the burn out stage resulted in powders with different crystalline phases. The PZT powder that was produced with route A gave a mixture of pyrochlore and perovskite phases. The powder that was produced with route B did not produce a detectable perovskite phase. These results indicate that an extra amount of PVP can delay the formation of the perovskite phase.

A similar comparison between XRD Fig. 6b and c shows that for the route B powder an increase in the burn out temperature and time produced a completely perovskite phase in the PZT. A comparison of the primary particles morphology in Figs. 4b and 5b indicates that the production of the perovskite phase was not at the expense of significant initial sintering of the powder. Figs. 4c and 5c show that the increase in the burn out temperature also effects the particle population. The average diameter of the sub-micron particles was increased. Particle formations with diameter above 1 μm were created. This behaviour can be explained by taking in consideration the local sintering that is noticeable in Fig. 5b. Fig. 5b shows that the particles with smother surfaces have also created bridges with their neighbour particles. These hard agglomerates would be correlated with the new population of micron-scale particles.

The role of the PVP in the sol–gel process was investigated using DSC. The common endothermic peak, in Fig. 7a and b, at 30–150 °C corresponds to the evaporation of the solvent and the water. The exothermic peak, at 310–370 °C, is common to all the PZT containing samples and is likely to correspond to the decomposition of the organic species. The exothermic peak exhibited by the PZT sol (Fig. 7a) between

420 and 450 °C is likely to be caused by the formation of a metastable pyrochlore phase accompanied by the remaining combustion of the organics.[33–35]

The endothermic peak at 420–450 °C exhibited by the PVP in Fig. 7a corresponds to the melting point of the polymer. Gel (i) also has an exothermic peak in the temperature range 420–450 °C but the total released energy was much greater than for the PZT sol sample. This indicates the presence of a different mechanism. The breaking of the hydrogen bonds between the C=O groups of PVP and the OH groups of the metalloxane polymers is likely to provided the extra energy. Gel (ii) exhibits the same behaviour as gel (i), except for an endothermic peak at 410–450 °C. The extra amount of polymer, added in the secondary stage, for gel (ii) is likely to account for this.

The DSC results indicate that the first stage polymer created bonds with the alkoxides and controlled the speed of the condensation reaction. However, the SEM pictures show that the first stage polymer was not able to prevent agglomeration during the drying process. The second stage polymer was necessary to complete the encapsulation of the first stage PZT particles and prevent them from further reaction during the drying and burn out stage.

5. Conclusions

Two sol–gel routes were used to create PZT powder. Both gave similar primary particles sizes and morphologies but different agglomerate formations. The extra amount of polymer that was added as a secondary stage prevented the formation of large agglomerates and created a powder with sub-micron primary particles. The amount of polymer in the PZT–PVP gel appears to be able to affect the final crystal phase of powder without affecting significantly the size of the freestanding particles.

Acknowledgements

This work would not have been possible without the financial support from EPSRC (grant no.: GR/R43303). The authors would like to thank Professor Roger Whatmore for his helpful discussion of the research results.

References

1. Rahaman, M. N., Ceramic Processing and Sintering, New York, 1995.
2. Junmin, X., Wang, J. and Weiseng, T., Synthesis of lead zirconate titanate from an amorphous precursor by mechanical activation. *J. Alloys Compd.*, 2000, **308**, 139–146.
3. Kong, L. B., Zhu, W. and Tan, O. K., Preparation and characterization of $Pb(Zr_{0.52}Ti_{0.48})O_3$ ceramics from high-energy ball milling powders. *Mater. Lett.*, 2000, **42**, 232–239.
4. Kong, L. B., Ma, J., Zhang, R. F., Zhu, W. and Tan, O. K., Lead zirconate titanate ceramics achieved by reaction sintering of PbO and high-energy ball milled $(ZrTi)O_2$ nanosized powders. *Mater. Lett.*, 2002, **55**, 370–377.
5. Brankovic, Z., Brankovic, G., Jovalekic, C., Maniette, Y. and Cilense, M., Mechanochemical synthesis of PZT powders. *Mater. Sci. Eng. A*, 2003, **345**, 243–248.
6. Das, R. N. and Pramanik, P., Chemical synthesis of nanocrystalline lead zirconate-titanate powders using tartarate precursor. *Mater. Lett.*, 1999, **40**, 251–254.
7. Das, R. N., Pati, R. K. and Pramanik, P., A novel chemical route for the preparation of nanocrystalline PZT powder. *Mater. Lett.*, 2000, **45**, 350–355.
8. Guo, Li, Lyashchenko, A. and Dong, X.-L., Synthesis of zirconium-rich PZT ceramics by hydroxide coprecipitation under hot-press. *Mater. Lett.*, 2002, **56**, 849–855.
9. Gang, Xu, Weng, W., Yao, J., Du, P. and Han, G., Low temperature synthesis of lead zirconate titanate powder by hydroxide co-precipitation. *Microelectr. Eng.*, 2003, **66**, 568–573.
10. Guiffard, B. and Troccaz, M., Low temperature synthesis of stoichiometric and homogeneous lead zirconate titanate powder by oxalate and hydroxide coprecipitation. *Mater. Res. Bull.*, 1998, **33**, 1759–1768.
11. Abothu, I. R., Shi-Fang, L., Komarneni, S. and Li, Q. H., Processing of $Pb(Zr_{0.52}Ti_{0.48})O_3$ (PZT) ceramics from microwave and conventional hydrothermal powders. *Mater. Res. Bull.*, 1999, **34**, 1411–1419.
12. Traianidis, M., Courtois, C. and Leriche, A., Mechanism of PZT crystallisation under hydrothermal conditions. Development of a new synthesis route. *J. Eur. Ceram. Soc.*, 2000, **20**, 2713–2720.
13. Traianidis, M., Courtois, C., Leriche, A. and Thierry, B., Hydrothermal synthesis of lead zirconium titanate (PZT) powders and their characteristics. *J. Eur. Ceram. Soc.*, 1999, **19**, 1023–1026.
14. Seung-Beom, C., Oledzka, M. and Riman, R. E., Hydrothermal synthesis of acicular lead zirconate titanate (PZT). *J. Cryst. Growth*, 2001, **226**, 313–326.
15. Fegley, B. and Barringer, E. A., Synthesis and characterisation of monosized doped TiO_2 powders. *J. Am. Ceram. Soc.*, 1984, **67**, 113–116.
16. Liu, X., An improvement on sol–gel method for preparing ultrafine and crystallized titania powder. *Mater. Sci. Eng. A*, 2000, **289**, 241–245.
17. An-Wu, X., The preparation, characterization, and their photocatalytic activities of rare-earth-doped TiO_2 nanoparticles. *J. Catal.*, 2002, **207**, 151–157.
18. Chuanfang, Y., Production of ultrafine ZrO_2 and Y-doped ZrO_2 powders by solvent extraction from solutions of perchloric and nitric acid with tri-*n*-butyl phosphate in kerosene. *Powder Technol.*, 1996, **89**, 149–155.
19. Suba, S.-I., Synthesis of $MgO–SiO_2$ and $CaO–SiO_2$ amorphous powder by sol–gel process and ion exchange. *J. Non-Cryst. Sol.*, 1999, **255**, 178–184.
20. Ogihara, T., Kaneko, H. and Mizutani, N., Preparation of monodispersed lead zirconate-titanate fine particles. *J. Mater. Sci. Lett.*, 1988, **7**, 867–869.
21. Zhou, Q. F., Nanocrystalline powder and fibres of lead zirconate titanate prepared by the sol–gel process. *J. Mater. Proc. Tech.*, 1997, **63**, 281–285.
22. Lakeman, C. D. E. and Payne, D. A., Processing effects in the sol–gel preparation of PZT dried gels, powders, and ferroelectric thin-layers. *J. Am. Ceram. Soc.*, 1992, **75**, 3091–3096.
23. Yang, W. D., PZT/PLZT ceramics prepared by hydrolysis and condensation of acetate precursors. *Ceram. Int.*, 2001, **27**, 373–384.
24. Weng, L., Bao, X. and Sagoe-Crentsil, K., Effect of acetylacetone on the preparation of PZT materials in sol–gel processing. *Mat. Sci. Eng. B*, 2002, **96**, 307–312.
25. Wang, F.-P., Yu, Y.-J., Jiang, Z.-H. and Zhao, L.-C., Synthesis of $Pb_{1-x}Eu_x(Zr_{0.52}Ti_{0.48})O_3$ nanopowders by a modified sol–gel process using zirconium oxynitrate source. *Mater. Chem. Phys.*, 2002, **77**, 10–13.

26. Brunckova, H., Medvecky, L., Briancin, J. and Saksi, K., Influence of hydrolysis conditions of the acetate sol–gel process on the stoichiometry of PZT powders. *Ceram. Int.*, 2004, **30**, 453–460.
27. Kozuka, H. and Higuchi, A., Single-layer submicron-thick $BaTiO_3$ coatings from PVP-containing sols: gel-to-ceramic film conversion, densification, and dielectric properties. *J. Mater. Res.*, 2001, **16**, 3116–3123.
28. Ho Rho, Y., Kanamura, K., Fujisaki, M., Hamagami, J.-I., Suda, S.-I. and Umegaki, T., Preparation of $Li_4Ti_5O_{12}$ and $LiCoO_2$ thin film electrodes from precursors obtained by sol–gel method. *Solid State Ionics*, 2002, **151**, 151–157.
29. Zheng, M.-P., Gu, M.-Y., Jin, Y.-P., Wang, H.-H., Zu, P.-F., Tao, P. *et al.*, Effects of PVP on structure of TiO_2 prepared by the sol–gel process. *Mater. Sci. Eng. B*, 2001, **87**, 197–201.
30. Rataboul, F., Nayral, C., Casanove, M.-J., Maisonnat, A. and Chaudret, B., Synthesis and characterization of monodisperse zinc and zinc oxide nanoparticles from the organometallic precursor $Zn(C_6H_{11})_2$. *J. Org. Chem.*, 2002, **643/644**, 307–312.
31. Kozuka, H. and Kajimura, M., Single-step dip coating of crack– ree $BaTiO_3$ films > 1 μm thick: effect of poly(vinylpyrrolidone) on critical thickness. *J. Am. Ceram. Soc.*, 2000, **83**, 1056–1062.
32. Kozuka, H. and Higuchi, A., Single-layer submicron-thick $BaTiO_3$ coatings from poly(vinylpyrrolidone)-containing sols: gel-to-ceramic film conversion, densification, and dielectric properties. *J. Mater. Res.*, 2001, **16**, 3116–3123.
33. Wu, A., Isabel, M., Salvado, M., Vilarinho, P. M. and Baptista, J. L., Lead zirconate titanate prepared from different zirconium and titanium precursors by sol–gel. *J. Am. Ceram. Soc.*, 1998, **81**, 2640–2644.
34. Chen, Y. Z., J.F M.A., Kong, L. B. and Zhang, R. F., Seeding in sol–gel process for $Pb(Zr_{0.52}Ti_{0.48})O_3$ powder fabrication. *Mater. Chem. Phys.*, 2002, **75**, 225–228.
35. Wu, A., Vilarinho, P. M., Miranda Salvado, I. M. and João, L. B., Sol–gel preparation of lead zirconate titanate powders and ceramics: effect of alkoxide stabilizers and lead precursors. *J. Am. Ceram. Soc.*, 2000, **83**, 1379–1385.